Hindawi
Wireless Communications and Mobile Computing
Volume 2021, Article ID 5528522, 10 pages
https://doi.org/10.1155/2021/5528522

Research Article

Dynamically Subarray-Connected Hybrid Precoding Scheme for Multiuser Millimeter-Wave Massive MIMO Systems

Guangyan Liao[1] **and Feng Zhao**[2]

[1]*Key Laboratory of Cognitive Radio and Information Processing, Guilin University of Electronic Technology, Guilin 541004, China*
[2]*Key Laboratory of Complex System Optimization and Big Data Processing, Guangxi Colleges and Universities, Yulin Normal University, Yulin 537000, China*

Correspondence should be addressed to Feng Zhao; zhaofeng@guet.edu.cn

Received 17 February 2021; Revised 7 April 2021; Accepted 19 April 2021; Published 28 April 2021

Academic Editor: Yan Huang

Hybrid precoding is widely used in millimeter wave (mmWave) massive multiple-input multiple-output (MIMO) systems. However, most prior work on hybrid precoding focused on the fully connected hybrid architectures and the subconnected but fixed architectures in which each radio frequency (RF) chain is connected to a specific subset of the antennas. The limited work shows that dynamic subarray architectures address the tradeoff between achievable spectral efficiency and energy efficiency of mmWave massive MIMO systems. Nevertheless, in the multiuser hybrid precoding systems, the existing dynamic subarray schemes ignore the fairness of users and the problem of user selection. In this paper, we propose a novel multiuser hybrid precoding scheme for dynamic subarray architectures. Firstly, we select a multiuser set among all users according to the analog effective channel information of the base station (BS) and then design the subset of the antennas to each RF by the fairness antenna-partitioning algorithm. Finally, the optimal analog precoding vector is designed according to each subarray, and the digital precoding is designed by the minimum mean-squared error (MMSE) criterion. The simulation results show that the performance advantages of the proposed multiuser hybrid precoding scheme for dynamic subarray architectures.

1. Introduction

Millimeter-wave massive MIMO, as a key technology in the next-generation wireless systems, can achieve multigigabit data rates benefiting from its abundant frequency resource [1] and provide highly directional beamforming gains to compensate for the path loss of mmWave signals [2]. For mmWave massive MIMO systems, hybrid precoding not only solves the problem that the fully digital precoding unsuitable for this systems, but also can achieve performance close to a full digital precoding [3, 4].

The studies of hybrid precoding focused on the fully connected architecture [5–8] and partially connected architecture [9–11], and there are two main ways to solve the hybrid precoding problem. One is the joint analog domain precoding and digital domain precoding simultaneously [5–7, 9]. And another is the analog domain precoding designed by the channel gain at first and then the digital domain precoding designed by the analog equivalent channel [12–15], and this way is usually applies to multiuser mmWave systems. However, most previous works did not explore the problem of the tradeoff between spectral efficiency and energy efficiency.

Limited works have been carried out for dynamic subarray-connected structures were proposed in [16–20]. This new structure is different from the previous structure, which uses a dynamic subarray connection structure to connect the RF chain and antenna according to the channel state information of the users. In [16], adaptive hybrid precoding (AHP) was developed to achieve the highest system spectral efficiency, but it is only applicable for the number of employed RF chains which is equal to the number of users. In [17], based on knowing the long-term channel characteristics, a technique of dynamically hybrid subarrays was developed, but the user's fairness was ignored. In [18], consider the number of RF chains which is more than or equal to that of

scheduled users and utilized AHP based on the singular value decomposition (SVD). However, that scheme does not study the problem of user selection when the number of users increases. Moreover, in [19], utilize the subchannel difference of the users, and a dynamically connected hybrid precoding was developed. This scheme allocates a different number of antennas for each RF chain, but sometimes some RF chains cannot allocate an antenna, which was unfair to some users. User selection was considered in [20], and a multiuser hybrid precoding framework based on codebooks was proposed, which adopted the antenna-partitioning algorithm based on the maximum increment of the signal-to-interference-noise ratio (SINR), but it has the same problem as [19].

In this paper, we proposed a new antenna-partitioning algorithm and hybrid analog/digital precoding schemes for the dynamic subarray characteristic. The main contributions of this paper can be summarized as follows.

(1) Proposing a new antenna-partitioning algorithm for multiuser mmWave system with a dynamic subarray characteristic. The algorithm guaranteed fairness because each user can obtain approximately equal channel gain. The new antenna-partitioning algorithm proposed in this paper avoids the problem that the number of antennas in some subarrays which is zero may occur in [20], and it can be used to the number of transmitting antennas and the number of subarrays which is not multiple. However, the AHP scheme in [16] is only applicable when the number of transmitting antennas is a multiple of the number of subarrays

(2) The dynamic hybrid structure model is obtained by the new antenna partition algorithm, which is based on the maximum channel gain of each user rather than SINR. Therefore, the spectrum efficiency of the system can be improved by eliminating the interuser interference through digital baseband precoding. Firstly, we design the analog precoding based on phase-only precoding. Then, in order to eliminate the interuser interference and ensure the high performance of the system under low SNR, we design the digital baseband precoding based on the minimum mean square error criterion. The simulation results show the advancement of our scheme

The remainder of the paper is as follows: Section 2 describes the multiuser massive MIMO system model and millimeter-wave channel model. The problem description is proposed in Section 3. Section 4 provides a detailed description of the proposed solution. Simulation results are presented in Section 5. Finally, conclusions are drawn in Section 6.

Notation. In this paper, we use the notation as the following: $\mathbf{X}$ is a matrix, $\mathbf{x}$ is a vector, and x is a scalar. $(\mathbf{X})^T$, $(\mathbf{X})^H$, and $(\mathbf{X})^\dagger$ denote the transpose, transpose-conjugate operation, and pseudo-inverse of $\mathbf{X}$, respectively. $\|\mathbf{X}\|_F$ and $|\mathbf{X}|$ denote the Frobenius norm and determinant of $\mathbf{X}$. $\mathrm{Tr}\{\mathbf{X}\}$ and $\mathbb{E}[\mathbf{X}]$ denote the trace and expectation of $\mathbf{X}$. $\mathcal{CN}(\mathbf{m}, \mathbf{R})$ is a complex Gaussian random vector with mean $\mathbf{m}$ and covariance $\mathbf{R}$.

2. System Model and Channel Model

2.1. System Model. In this study, we describe three different multiuser hybrid precoding system models, the fully connected structures, the subconnected structures, and the dynamic subarray structures. Firstly, a fully connected multiuser downlink massive MIMO hybrid precoding system models as shown in Figure 1, where the BS is equipped with N_{RF} RF chains and N_T antennas. We assume that the BS simultaneously communicates with K mobile users. Each mobile user is equipped with one RF chain and N_R antennas, where $K \le N_{\mathrm{RF}} \le N_T$. The BS antennas are tagged as 1,2, …, N_T, and let $\Xi = \{1, 2, \cdots, N_T\}$. The baseband precoding matrix $\mathbf{F}_{\mathrm{BB}} = [\mathbf{F}_{\mathrm{BB}}^1, \mathbf{F}_{\mathrm{BB}}^2, \cdots, \mathbf{F}_{\mathrm{BB}}^K]$, where $\mathbf{F}_{\mathrm{BB}}^k \in \mathbb{C}^{N_{\mathrm{RF}} \times N_R}$ is the baseband precoding matrix for k th mobile user. The analog precoding weight is a $N_T \times N_{\mathrm{RF}}$ matrix $\mathbf{F}_{\mathrm{RF}} = [\mathbf{f}_{\mathrm{RF}}^1, \mathbf{f}_{\mathrm{RF}}^2, \cdots, \mathbf{f}_{\mathrm{RF}}^{N_{\mathrm{RF}}}]$, where $\mathbf{f}_{\mathrm{RF}}^k \in \mathbb{C}^{N_T \times 1}$ is the analog precoding vector for the k th RF chain. $\mathbf{F}_{\mathrm{RF}}$ and $\mathbf{F}_{\mathrm{BB}}$ are linked by the total power constrains, i.e, $\|\mathbf{F}_{\mathrm{RF}}\mathbf{F}_{\mathrm{BB}}\|_F^2 = K$. The sample transmitted signal can be represented as [21].

$$\mathbf{x} = \mathbf{F}_{\mathrm{RF}}\mathbf{F}_{\mathrm{BB}}\mathbf{s}, \tag{1}$$

where $\mathbf{s} = [s_1, s_2, \cdots, s_K]^T$ is the $K \times 1$ vector of transmitted symbols, which satisfy $\mathbb{E}[\mathbf{s}\mathbf{s}^H] = (P/K)\mathbf{I}_K$, and P is the average total transmitted power.

Generally, the received downlink signal of the mobile user k can be represented as [21].

$$\mathbf{y}_k = \mathbf{w}_k\mathbf{H}_k\mathbf{F}_{\mathrm{RF}}\mathbf{f}_{\mathrm{BB}}^k s_k + \sum_{i \ne k}\mathbf{w}_k\mathbf{H}_k\mathbf{F}_{\mathrm{RF}}\mathbf{f}_{\mathrm{BB}}^i s_i + \mathbf{w}_k\mathbf{n}_k, \tag{2}$$

where $\mathbf{H}_{\mathrm{k}} \in \mathbb{C}^{N_R \times N_T}$ is the channel matrix from the BS to the k th mobile user. Let $\mathbf{H} = [\mathbf{H}_1, \mathbf{H}_2, \cdots, \mathbf{H}_N]^T$. $\mathbf{n}_k$ is an additive Gaussian white noise vector such that $\mathbf{n}_k \sim \mathcal{CN}(\mathbf{0}, \delta^2\mathbf{I})$. $\mathbf{w}_{\mathrm{k}} \in \mathbb{C}^{1 \times N_R}$ denotes the digital vector at the k th mobile user.

Then, we describe the two structures shown in Figure 2 and define the form of their analog precoding matrices. The conventional subarray architecture in which each RF chain is connected to a specific subset of the antennas as shown in Figure 2(a), and each RF chain connected to the antenna is fixed in the order. Therefore, we can define the analog precoding matrix $\mathbf{F}_{\mathrm{RF}}$ as [9].

$$\mathbf{F}_{\mathrm{RF}} = \begin{bmatrix} \mathbf{f}_{\mathrm{RF}}^1 & \mathbf{0} & \cdots & \mathbf{0} \\ \mathbf{0} & \mathbf{f}_{\mathrm{RF}}^2 & & \mathbf{0} \\ \vdots & & \ddots & \vdots \\ \mathbf{0} & \mathbf{0} & \cdots & \mathbf{f}_{\mathrm{RF}}^{N_{RF}} \end{bmatrix}_{N_{RF}M \times N_{\mathrm{RF}}}, \tag{3}$$

where $\mathbf{f}_{\mathrm{RF}}^j = [f_j^{(j-1)M+1}, f_j^{(j-1)M+2}, \cdots, f_j^{jM}]^T$ denotes the analog weighting vector for the j th RF chain, $M = N_T/N_{\mathrm{RF}}$, and $j = 1, 2, \cdots, N_{\mathrm{RF}}$.

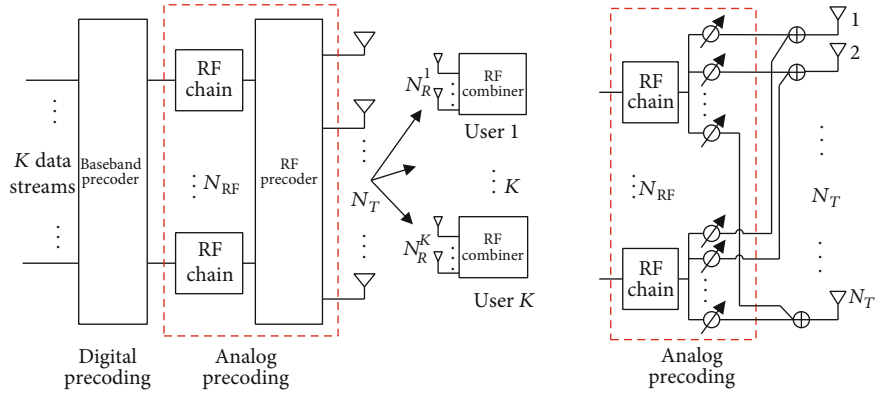

Figure 1: Fully connected architecture of the multiuser hybrid precoding in mmWave massive MIMO system.

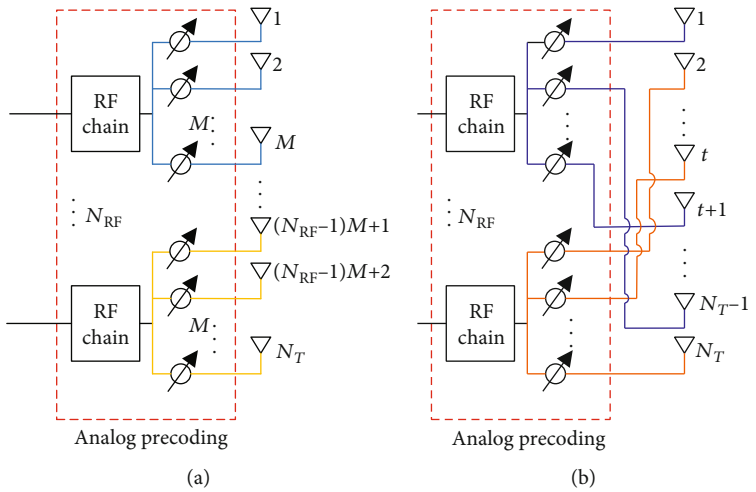

Figure 2: Two subconnected architectures of the multiuser hybrid precoding in mmWave massive MIMO system: (a) conventional subarray architecture, where each RF chain is connected to a fixed subset of the antennas; (b) dynamic subarray architecture, where each RF chain is connected to interlaced antennas.

The dynamic subarray architectures are shown in Figure 2(b), which each RF chain is connected to a dynamic subset of the antennas. The analog precoding matrix $\mathbf{F}_{RF} = [\mathbf{f}_{RF}^{S_1}, \mathbf{f}_{RF}^{S_2}, \cdots, \mathbf{f}_{RF}^{S_{N_{RF}}}]$ is derived with

$$\mathbf{f}_{RF}^{S_j}(t,j) = \begin{cases} f_j^t, t \in S_j, \\ 0, t \notin S_j, \end{cases} \tag{4}$$

where $\mathbf{f}_{RF}^{S_j} \in \mathbb{C}^{N_T \times 1}$ is the analog precoding vector for the j th RF chain, and $\mathbf{f}_{RF}^{S_j}(t,j)$ denotes the element of t th antenna connected to the j th RF chain. Assume that f_j^t is a value of $\mathbf{f}_{RF}^{S_j}(t,j)$. The set S_j contains label of antenna connected to the j th RF chain, and let set $S = \{S_1, S_2, \cdots, S_j, \cdots, S_{N_{RF}}\}$, $\sum_{j=1}^{N_{RF}} |S_j| = N_T$.

2.2. mmWave Channel Model. Millimeter wave channels with high free-space path loss and large dense antenna arrays are unlikely to follow the rich scattering model at low frequencies. According to the characteristics of millimeter wave propagation, the dense array makes the antenna highly correlated, and the high path loss in high free-space leads to the limited space selectivity. Thus, the millimeter-wave channel is considered to have finite scattering [1]. Traditional MIMO channel modeling methods are not accurate in millimeter wave channel. The geometric channel model can embody the low rank and spatial correlation characteristics of mmWave communications [9]. Thus, we consider a geometric channel model with L_k scatterers for the k th user and assume that each scatterer contributes a single propagation path between the BS and the user [18, 21]. Under this model, the k th user's channel can be represented as

$$\mathbf{H}_k = \sqrt{\frac{N_T N_R}{L_k}} \sum_{l=1}^{L_k} \beta_{l,k} \mathbf{a}_R\left(\theta_{l,k}^R\right) \mathbf{a}_T^H\left(\theta_{l,k}^T\right), \tag{5}$$

where L_k is the number of scatterers and $\beta_{l,k}$ is the complex

gain of the l th path between the BS and the k th user. $\theta_{l,k}^{\mathrm{R}}$ and $\theta_{l,k}^{\mathrm{T}}$, respectively, represent the azimuth of arrival (AOA) and departure (AOD) of the l th path between the BS and the k th user, and the range of values for both $\theta_{l,k}^{\mathrm{R}}$ and $\theta_{l,k}^{\mathrm{T}}$ is $[0, 2\pi]$. $\mathbf{a}_T(\theta_{l,k}^{\mathrm{T}})$ and $\mathbf{a}_{\mathrm{R}}(\theta_{l,k}^{\mathrm{R}})$ are the antenna array response vectors of the base station and k th user, separately. For a uniform linear array (ULA), the array response vector can be written as

$$\mathbf{a}_{\mathrm{T}}\left(\theta_{l,k}^{\mathrm{T}}\right) = \frac{1}{\sqrt{N_T}}\left[1, e^{j(2\pi d/\lambda)\ \sin\ \left(\theta_{l,k}^{\mathrm{T}}\right)}, \cdots, e^{j(N_T-1)(2\pi d/\lambda)\ \sin\ \left(\theta_{l,k}^{\mathrm{T}}\right)}\right]^T, \tag{6}$$

where λ is the signal wavelength and $d = \lambda/2$ denotes the spacing distance between two adjacent antennas. The array response vector $\mathbf{a}_{\mathrm{R}}(\theta_{l,k}^{\mathrm{R}})$ takes a similar fashion.

3. Problem Formulation

In this section, we propose the problem of multiuser hybrid precoding scheme based on dynamic subarray architectures. As shown in Figure 2(b), the antennas of each subarray are not adjacent to each other, and the optimal set S^* needs to get at first. Then, design the hybrid precoding matrix $\mathbf{F}_{\mathrm{RF}}$ and $\mathbf{F}_{\mathrm{BB}}$ for the dynamic subarray architectures at the BS. In this paper, we assume that the channel state information (CSI) is perfect. The SINR of the k th user is written as

$$\mathrm{SINR}_k = \frac{P\left\|\tilde{\mathbf{H}}_k\mathbf{F}_{\mathrm{RF}}\mathbf{f}_{\mathrm{BB}}^k\right\|_F^2}{K\sigma_k^2 + P\sum_{i\neq k}\left\|\tilde{\mathbf{H}}_k\mathbf{F}_{\mathrm{RF}}\mathbf{f}_{\mathrm{BB}}^i\right\|_F^2}, \tag{7}$$

where $\tilde{\mathbf{H}}_k = \mathbf{w}_k\mathbf{H}_k$, and $\mathbf{w}_k = \mathbf{U}_k^H$ is obtained by SVD of $\mathbf{H}_k$, which is $\mathbf{H}_k = \mathbf{U}_k\mathbf{\Lambda}_k\mathbf{V}_k^H$.

The achievable rate of the k th user can be written as

$$R_k = \log_2(1 + \mathrm{SINR}_k). \tag{8}$$

We aim to jointly design the S^*, $\mathbf{F}_{\mathrm{RF}}^*$, and $\mathbf{F}_{\mathrm{BB}}^*$ to maximize the achievable sum-rate of dynamic subarray architectures, which can be formulated as

$$\begin{aligned}\{S^*, \mathbf{F}_{\mathrm{RF}}^*, \mathbf{F}_{\mathrm{BB}}^*\} &= \arg\max_{\mathbf{F}_{\mathrm{RF}}, \mathbf{F}_{\mathrm{BB}}, S}\sum_{k=1}^{K}\log_2(1 + \mathrm{SINR}_k),\\ s.t. \left\|\mathbf{f}_{\mathrm{RF}}(t,j)\right\|_F^2 &= 1, t = 1, 2, \cdots, N_T,\\ \left\|\mathbf{F}_{\mathrm{RF}}\mathbf{F}_{\mathrm{BB}}\right\|_F^2 &= K.\end{aligned} \tag{9}$$

The optimization problem of (9) is a nonconvex problem, and it is almost impossible to solve the global optimal solution directly. We decompose problem (9) into three subproblems. Firstly, we design the initial precoding matrix for each user to get the optimal set S^*. Secondly, we design the optimal analog precoding matrix $\mathbf{F}_{\mathrm{RF}}^*$ according to S^*, and finally, we design the optimal digital precoding matrix $\mathbf{F}_{\mathrm{BB}}^*$ through the equivalent channel matrix $\widehat{\mathbf{H}}_k = \tilde{\mathbf{H}}_k\mathbf{F}_{\mathrm{RF}}$. The detail of the scheme will be explained in the next section.

4. Hybrid Precoding Strategy

In this section, we introduce a dynamically subarray-connected hybrid precoding scheme for multiuser mmWave massive MIMO systems, including analog precoding initialization and user selection, dynamic antenna partitioning, and the hybrid precoding optimize for the dynamic subarray structures.

4.1. Initialization Analog Precoding and User Selection. In the multiuser mmWave massive MIMO system, the mmWave channel has a finite number of strong beam directions; thus, the best beams of the users lie on their own scattering paths. When the base station serves all users in the same time slot, the performance of the system will be degraded with the increase of interuser interference. Increasing the number of served users at the same time slot will result in performance degradation [22, 23]. In this paper, we select a group of users with minimum interuser interference and maximum objective channel gains. Generally, maximizing the SINR is the criterion for user selection [15].

Firstly, we define a set of all candidate users $\mathcal{N} = \{1, 2, \cdots, N\}$ and an empty set $\mathcal{U}$. The initial analog precoding vector $\mathbf{f}_n^0$ of n th user ($n = 1, 2, \cdots, N$) can be obtained by solving

$$\begin{aligned}\mathbf{f}_n^0 &= \arg\max \left\|\mathbf{H}_n\mathbf{f}_n\right\|_F^2,\\ s.t. \left|\mathbf{f}_n(t,n)\right| &= 1, \forall n, t.\end{aligned} \tag{10}$$

The SVD of channel $\mathbf{H}_n$ can be expressed as $\mathbf{H}_n = \mathbf{U}_n\mathbf{\Lambda}_n\mathbf{V}_n^H$. The unconstrained analog precoding vector for user n can be written as $\mathbf{f}_n^{\mathrm{opt}} = \mathbf{v}_n^1$, where $\mathbf{v}_n^1$ is the first columns of $\mathbf{V}_n$.

The optimization problem (10) can be rewritten as

$$\begin{aligned}\mathbf{f}_n^0 &= \arg\min \left\|\mathbf{f}_n^{\mathrm{opt}} - \mathbf{f}_n\right\|_F^2,\\ s.t. \left|\mathbf{f}_{\mathrm{RF}}(t,n)\right| &= 1, \forall n, t.\end{aligned} \tag{11}$$

The solutions of similar problems with (11) are given in [9]. Therefore, the solution of (11) can be obtained directly.

$$\mathbf{f}_n^0 = e^{j\angle\mathbf{f}_n^{\mathrm{opt}}} = e^{j\angle\mathbf{v}_n^1}. \tag{12}$$

Then, the process of multiuser selection is described as follows. Using the initial analog precoding vectors, the SINR of the user n written as

$$\mathrm{SINR}_n = \frac{P\left\|\mathbf{w}_n\mathbf{H}_n\mathbf{f}_n^0\right\|_F^2}{K\sigma_n^2 + P\sum_{i\neq n}\left\|\mathbf{w}_n\mathbf{H}_n\mathbf{f}_i^0\right\|_F^2}. \tag{13}$$

The first user $\mathcal{U}(1)$ selected by maximum channel gain $\left\|\mathbf{w}_n\mathbf{H}_n\right\|_F^2$ from set $\mathcal{N}$, and then, we update both set $\mathcal{N}$ and $\mathcal{U}$. The remaining users are selected from all candidate users set $\mathcal{N}$ according to the maximum SINR criterion, which can be described as follows:

$$\mathcal{U}(k) = \arg\max_{\mathcal{N},\mathcal{U}} \frac{P\left\|\mathbf{w}_{\mathcal{N}(n)}\mathbf{H}_{\mathcal{N}(n)}\mathbf{f}^0_{\mathcal{N}(n)}\right\|_F^2}{K\sigma^2_{\mathcal{N}(n)} + P\sum_{i=1}^{k-1}\left\|\mathbf{w}_{\mathcal{N}(n)}\mathbf{H}_{\mathcal{N}(n)}\mathbf{f}^0_{\mathcal{U}(i)}\right\|_F^2},$$
$$k \le K \le N_{\mathrm{RF}},\ i = 1, 2, \cdots, k-1, \tag{14}$$

where $\mathbf{H}_{\mathcal{N}(n)}$ is the mmWave channel of the n th user in set $\mathcal{N}$, $\mathbf{f}^0_{\mathcal{N}(n)}$ and $\mathbf{f}^0_{\mathcal{U}(i)}$ denote the initial analog precoding vector of the n th user in set $\mathcal{N}$ and the initial analog precoding vector of the i th user in set $\mathcal{U}$, respectively. The user $\mathcal{U}(k)$ with maximum SINR value is removed from $\mathcal{N}$ and added to $\mathcal{U}$. The update strategy is as follows:

$$\mathcal{U} \longleftarrow \mathcal{U} \cup \mathcal{U}(k), \mathcal{N} \longleftarrow \mathcal{N} \setminus \mathcal{U}(k). \tag{15}$$

The process of multiuser selection is summarized in Algorithm 1.

4.2. Dynamic Subarray for Multiuser mmWave System. The dynamic subarray hybrid architecture is a more efficient structure, in which the antenna elements are dynamically partitioned to each RF chain based on the long-term channel information [16, 18], and it addresses the tradeoff between the achievable spectral efficiency and energy efficiency. The existing antenna partition algorithm for dynamic subarray hybrid architecture is proposed in [20], but it has poor user fairness because of insufficient conditions. It uses the maximum increment of the SINR for each selected user, the conditions to ensure that each RF chain can be allocated one antenna at least have not been set, resulting in some RF chains not being partition of any antenna under special circumstances, such as some users can obtain the maximum SINR increment in all loop. In this subsection, based on the dynamic subarray hybrid structure proposed in Section 2, we design the new antenna partition algorithm to obtain higher spectral efficiency and guarantee user fairness.

The objective of this subsection is to address the optimal S_k^* of the user k. We assume that the number of chain N_{RF} is equal to the number of user K, and the BS transmits data to every user via only one stream. As shown in Figure 2(b), there are two constraints as

$$\sum_{j=1}^{N_{\mathrm{RF}}} |\mathbf{f}_{\mathrm{RF}}(t, j)| = 1, \tag{16}$$

$$\sum_{t=1}^{N_T} |\mathbf{f}_{\mathrm{RF}}(t, j)| \ge N, \tag{17}$$

where $N = (N_T - N_T \bmod N_{\mathrm{RF}})/N_{\mathrm{RF}}$, and the constrain of (16) ensures that each antenna is only connected to one RF chain, and the constrain of (17) ensures that each RF chain is connected to N antennas at least.

Then, in order to ensure that each user gets maximize channel gain and ensure fairness among users, we neglect the resulting interference among users in this stage, and the user interference elimination problem is solved in the next subsection. Directly solving three unknown matrix variables S^*, $\mathbf{F}^*_{\mathrm{RF}}$, and $\mathbf{F}^*_{\mathrm{BB}}$ will lead to high computational complexity. Therefore, we use the initial analog precoding vectors as significant information for partitioning antenna elements and let the dynamic subarray of each user start out as an empty set. The antenna-partitioning problem is described as

$$t^* = \arg\max_{t \in \Xi} \left\|\mathbf{w}_k\mathbf{H}_k\mathbf{f}^0_{S_k \cup t}\right\|_F^2, \tag{18}$$

where $\mathbf{f}^0_{S_k}$ is a $N_T \times 1$ vector, which is obtained by $\mathbf{f}^0_k$ according to (4), and $S_k \cup t$ represents the antenna t being added to the subarray S_k of k th user. Then, set Ξ and subarray S_k are updated as follows:

$$S_k \longleftarrow S_k \cup t^*, \Xi \longleftarrow \Xi \setminus t^*, \tag{19}$$

Within each inner loop of Algorithm 2, due to the constrain in (17), (18), and (19), will be carried out for all users once, and this inner loop will be carried out for N times. After the N loop, if $\Xi \neq \varnothing$, it means that there are still remaining antennas unallocated, and we allocate the remaining antennas to the user with the smallest channel gain. The details of the process are described in Algorithm 2.

For the simplicity of the process analysis, we assume that the number of chain N_{RF} is equal to the number of user K, and the BS transmits data to every user via only one stream. In fact, by changing the constraints (16) and (17), this new antenna partition algorithm can easily be extended to user multistream transmission.

4.3. Hybrid Precoding Design. In this subsection, we will design the hybrid precoding for dynamic subarray hybrid architecture that obtained in the previous subsection. For the dynamic subarray hybrid architecture, the beam shape and width are changed after the antenna partitioning of this architecture, and the initial analog precoding vector is invalid. Therefore, the analog precoding needs to be redesigned.

Utilize the subarray $S_1, S_2, \cdots, S_K$, the channel matrix for each user can be updated as

$$\mathbf{H}_k^{S_k}(:, t) = \begin{cases} \mathbf{H}_k(:, t), & t \in S_k, \\ 0, & t \notin S_k, \end{cases}$$
$$\bar{\mathbf{H}}_k = \mathbf{H}_k^{S_k}, \tag{20}$$

where $\bar{\mathbf{H}}_k$ is a $N_R \times N_T$ channel matrix for k th user, and define the effective channel $\mathbf{e}_k = \mathbf{w}_k\bar{\mathbf{H}}_k$ for k th user, where $\mathbf{w}_k$ can obtain by SVD of $\bar{\mathbf{H}}_k$.

In order to obtain the large array gain, we consider the phase-only control at the RF domain [24] and perform the analog precoding for each user according to

$$\mathbf{f}_k^{S_k} = e^{j(-\varphi_k)}, \tag{21}$$

where φ_k is the phase of the k th element in the vector $\mathbf{e}_k$ and $-\varphi_k$ is the conjugate transpose of φ_k.

1:Input: $\mathbf{H}$, $\mathcal{N}$, $\mathcal{U}$, K
2:Initialize: $\mathbf{H} = [\mathbf{H}_1, \mathbf{H}_2, \cdots, \mathbf{H}_N]^T$, $\mathcal{N} = \{1, 2, \cdots, N\}$, $\mathcal{U} = \varnothing$
3:for $\mathbf{n} = \mathbf{1}:\mathbf{N}$ do
4: Calculate the SVD of $\mathbf{H}_n$ to obtain $\mathbf{W}_n$ and $\mathbf{V}_n$, $\mathbf{w}_n = W_n^H(1, :)$, $\mathbf{f}_n^0 = e^{j\angle \mathbf{v}_n^1}$, where $\mathbf{v}_n^1$ is the first columns of $\mathbf{V}_n$.
5: $\nabla_n = \|\mathbf{w}_n \mathbf{H}_n\|_F^2$
6:end for
7: $\mathcal{U}(1) = \arg\max_{\mathcal{N}} \nabla_n$
8: $\mathcal{U} \longleftarrow \mathcal{U} \cup \mathcal{U}(1), \mathcal{N} \longleftarrow \mathcal{N} \setminus \mathcal{U}(1)$
9:for $\mathbf{k} = \mathbf{2}:\mathbf{K}$ do
10: $\mathcal{U}(k) = \arg\max_{\mathcal{N},\mathcal{U}} (P\|\mathbf{w}_{\mathcal{N}(n)} \mathbf{H}_{\mathcal{N}(n)} \mathbf{f}_{\mathcal{N}(n)}^0\|_F^2 / K\sigma_{\mathcal{N}(n)}^2 + P\sum_{i=1}^{k-1} \|\mathbf{w}_{\mathcal{N}(n)} \mathbf{H}_{\mathcal{N}(n)} \mathbf{f}_{\mathcal{U}(i)}^0\|_F^2)$
11: $\mathcal{U} \longleftarrow \mathcal{U} \cup \mathcal{U}(k), \mathcal{N} \longleftarrow \mathcal{N} \setminus \mathcal{U}(k)$
12:end for
13:output: $\mathcal{U}$

Algorithm 1: Multiuser selection based on SINR.

1:Input: $\mathbf{H}$, $\mathcal{U}$, K, $S = \{S_1, S_2, \cdots, S_k, \cdots, S_K\}$, $\mathbf{f}_n^0$
2:Initialize: $\mathbf{H} = [\mathbf{H}_1, \mathbf{H}_2, \cdots, \mathbf{H}_N]^T$, $\mathcal{U}$ and $\mathbf{f}_n^0$ are obtain by Algorithm 1, $K = |\mathcal{U}|$, $S_1 = S_2 = \cdots = S_K = \varnothing$, $N = (N_T - N_T \bmod N_{\mathrm{RF}})/N_{\mathrm{RF}}$
3:for loop = $\mathbf{1}:\boldsymbol{N}$ do
4: for $\mathbf{k} = \mathbf{1}:\mathbf{K}$ do
5: $t^* = \arg\max_{t \in \Xi} \|\mathbf{w}_k \mathbf{H}_k \mathbf{f}_{S_k \cup t}^0\|_F^2$
6: $S_k \longleftarrow S_k \cup t^*, \Xi \longleftarrow \Xi \setminus t^*$
7: $\Delta_k = \|\mathbf{w}_k \mathbf{H}_k \mathbf{f}_{S_k}^0\|_F^2$
8: end for
9:end for
10:while $\Xi \neq \varnothing$ do
11: $k^* = \arg\min_{k=1,\cdots,K} \Delta_k$
12: $t^* = \arg\max_{t \in \Xi} \|\mathbf{w}_{k^*} \mathbf{H}_{k^*} \mathbf{f}_{S_{k^*} \cup t}^0\|_F^2$
13: $S_{k^*} \longleftarrow S_{k^*} \cup t^*, \Xi \longleftarrow \Xi \setminus t^*$
14: $\Delta_{k^*} = \|\mathbf{w}_{k^*} \mathbf{H}_{k^*} \mathbf{f}_{S_{k^*}}^0\|_F^2$
15:end while
16:output: $S_1, S_2, \cdots, S_K$

Algorithm 2: Multiuser dynamic subarray partitioning.

In the stage of digital baseband precoding, we focused on the elimination of interuser interference. Some classical digital precoding algorithms are used to eliminate the interuser interference, such as ZF and BD. However, in multiuser systems with a low signal-to-noise ratio (SNR), ZF or BD precoding performs poorly [12]. Thus, we use the minimum mean-squared error criteria to design digital baseband precoding. According to the received signal model in (2), the estimated symbol of k th user is given by

$$\widehat{s}_k = \mathbf{w}_k \bar{\mathbf{H}}_k \mathbf{F}_{\mathrm{RF}} \mathbf{F}_{\mathrm{BB}}^k s_k + \mathbf{w}_k \bar{\mathbf{H}}_k \sum_{i \neq k}^{K} \mathbf{F}_{\mathrm{RF}} \mathbf{F}_{\mathrm{BB}}^i s_i + \mathbf{w}_k \mathbf{n}_k. \tag{22}$$

The estimated symbols for all users given (22) can be stacked into one vector.

$$\widehat{\mathbf{s}} = \mathbf{W} \bar{\mathbf{H}} \mathbf{F}_{\mathrm{RF}} \mathbf{F}_{\mathrm{BB}} \mathbf{s} + \mathbf{W}\mathbf{n}, \tag{23}$$

where $\bar{\mathbf{H}} = [\bar{\mathbf{H}}_1^T, \bar{\mathbf{H}}_2^T, \cdots, \bar{\mathbf{H}}_K^T]^T$, $\mathbf{W} = \mathrm{blkdiag}(\mathbf{w}_1, \mathbf{w}_2, \cdots, \mathbf{w}_K)$, $\mathbf{F}_{\mathrm{RF}} = [\mathbf{f}_1^{S_1}, \mathbf{f}_2^{S_1}, \cdots, \mathbf{f}_K^{S_K}]$, $\mathbf{F}_{\mathrm{BB}} = \mathrm{blkdiag}(\mathbf{F}_{\mathrm{BB}}^1, \mathbf{F}_{\mathrm{BB}}^2, \cdots, \mathbf{F}_{\mathrm{BB}}^K)$, and $\mathbf{n} = [\mathbf{n}_1^T, \mathbf{n}_2^T, \cdots, \mathbf{n}_K^T]^T$. The aim is to get estimated symbols $\widehat{\mathbf{s}}$ close to $\mathbf{s}$. The mean-squared error cost function can be expanded as

$$\begin{aligned} \mathbb{E}\left[\|s - \sqrt{\gamma}\mathbf{s}\wedge\|^2\right] &= \mathbb{E}\left[\left\|s - \sqrt{\gamma}\mathbf{W}\bar{\mathbf{H}}\mathbf{F}_{\mathrm{RF}}\mathbf{F}_{\mathrm{BB}}\mathbf{s} - \sqrt{\gamma}\mathbf{W}\mathbf{n}\right\|^2\right] \\ &= \left\|\mathbf{I}_K - \mathbf{W}\bar{\mathbf{H}}\mathbf{F}_{\mathrm{RF}}\mathbf{F}_{\mathrm{BB}}\right\|_F^2 + K\gamma\sigma^2, \end{aligned} \tag{24}$$

where γ is the scaling factor.

Then, the problem of minimum mean-squared error can be expressed as

$$\underset{\mathbf{F}_{\mathrm{RF}}, \mathbf{F}_{\mathrm{BB}}, \gamma}{\text{minimize}} \ \left\|\mathbf{I}_K - \mathbf{W}\bar{\mathbf{H}}\mathbf{F}_{\mathrm{RF}}\mathbf{F}_{\mathrm{BB}}\right\|_F^2 + K\gamma\sigma^2 s.t. \quad \mathrm{Tr}\left\{\mathbf{F}_{\mathrm{RF}}^H \mathbf{F}_{\mathrm{RF}} \mathbf{F}_{\mathrm{BB}} \mathbf{F}_{\mathrm{BB}}^H\right\} \leq \gamma P. \tag{25}$$

The analog precoding matrix $\mathbf{F}_{\mathrm{RF}}$ can be obtained by (21); thus, the problem (25) will be transformed into a convex optimization problem. The closed-form optimal solution of the similar problem is given in [25]. Its optimal solution is given by

$$\mathbf{F}_{\mathrm{BB}} = \left(\mathbf{T}^H\mathbf{T} + \frac{K\delta^2}{P}\mathbf{I}_K\right)^{\dagger}\mathbf{T}^H, \tag{26}$$

where $\mathbf{T} = \mathbf{W}\bar{\mathbf{H}}\mathbf{F}_{\mathrm{RF}}$, the optimal scaling factor $\gamma = \|\mathbf{F}_{\mathrm{RF}}\mathbf{F}_{\mathrm{BB}}\|_F^2/P$, normalizes $\mathbf{F}_{\mathrm{BB}} = \sqrt{1/\gamma}\mathbf{F}_{\mathrm{BB}}$.

In the process of MMSE-based digital precoding computation, the main computational complexity comes from formula (26). In (26), the complexity of matrix multiplication is $\mathcal{O}(K^2N_RN_TN_{\mathrm{RF}})$, and the complexity of pseudo-inverse is $\mathcal{O}(K^3)$. Therefore, the total complexity is $\mathcal{O}(K^2N_RN_TN_{\mathrm{RF}} + K^3)$. Since the baseband digital precoding design in hybrid precoding is carried out in low dimensions, the increase in the number of base station transmitting antennas will not bring huge computational complexity. In practical application, this method may bring some challenges when the number of users increases rapidly. In general, the MMSE-based baseband digital precoding is an effective method.

5. Simulation Results

In this section, simulation results are given to illustrate the performance advantages of the proposed new antenna-partitioning algorithm and hybrid analog/digital precoding scheme in spectrum efficiency, energy efficiency, and user fairness. We compare the performance of three hybrid precoding schemes with different structures, namely, conventional subconnected structure, existing dynamic subarray-connected structure [20], and fully connected structure. Firstly, we consider a mmWave channel and dynamic subarray architecture described in Section 2. The carrier frequency is set as 28 GHz [1]. The number of scatterers for each user is $L_k = 3$. The transmit antenna arrays are ULAs with antenna spacing $d = \lambda/2$. We assume that both the AoAs and AoDs are following the uniform distribution within $[-\pi, \pi]$. Finally, SNR is defined P/σ^2.

5.1. Performance Comparisons of Spectrum Efficiency. Figure 3 shows the spectral efficiency comparison in different architectures, where the BS is equipped with 64 antennas and 2 RF chains serving two users, and each user is equipped with two antennas. We observe from Figure 3 that the performance of the proposed new antenna-partitioning-based hybrid precoding scheme outperforms the existing dynamic subarray precoding scheme [20] in the whole simulated SNR range. For instance, when SNR = 0 dB, our proposed scheme can achieve 86.1% of the spectral efficiency obtained by fully connected architecture, and compared with the conventional subarray architecture, the spectral efficiency of the proposed scheme is improved by 11.1%. Moreover, compared with the existing dynamic subarray architecture scheme, the spectral efficiency of the proposed scheme is also

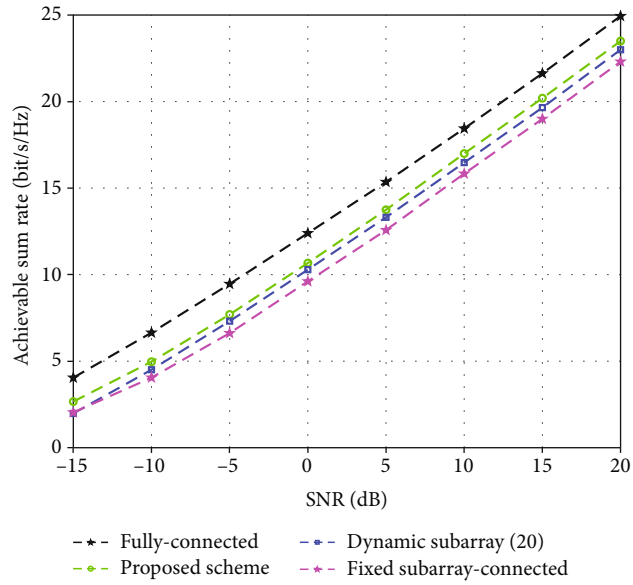

Figure 3: Spectral efficiency comparison for the mmWave MIMO system with $N_T = 64$, $N_R = 2$, $K = 2$, and $N_{\mathrm{RF}} = 2$ RF chains.

improved; especially at low SNR, the spectral efficiency is improved by 4.7% when SNR = 0 dB.

In Figure 4, the BS is equipped with 128 antennas and 2 RF chains serving two users. Similar to the trend in Figure 3, the spectrum efficiency of all architectures is improved, and our proposed scheme is still superior to the existing dynamic subarray architecture scheme. As can be seen from Figures 3 and 4, our proposed scheme is closer to the performance achieved by fully connected architecture, and the advantages are obvious at low SNR.

Figure 5 provides a spectrum efficiency comparison against the number of BS transmitting antennas. The BS is equipped with different antennas and two RF chains serving two users. As observed form Figure 5, the spectral efficiency increases with the increase of the number of antennas, but the rate of increase slows down when the SNR = −10 dB and the SNR = 0 dB. More importantly, the existing dynamic subarray schemes [20] do not show significant advantages when the BS equipped small transmitting antennas, such as 16 and 32. Moreover, our proposed scheme in this paper has obvious advantages in the whole simulation range.

5.2. Performance Comparisons of Energy Efficiency. The energy consumption model was proposed in [26], and based on this model, the energy efficiency η can be defined as

$$\eta = \frac{R_{\mathrm{sum}}}{P_{\mathrm{total}}} = \frac{\sum_{k=1}^{K}\log_2(1+\mathrm{SINR}_k)}{P_t + N_{\mathrm{RF}}P_{\mathrm{RF}} + N_{\mathrm{PS}}P_{\mathrm{PS}}}\,(\mathrm{bps/Hz/W}), \tag{27}$$

where P_{total} is the total energy consumption, P_t is the transmission power, P_{RF} is the energy consumed by RF chain, and P_{PS} is the energy consumed by phase shifter. N_{RF} and N_{PS} are the number of required RF chains and phase shifters, respectively.

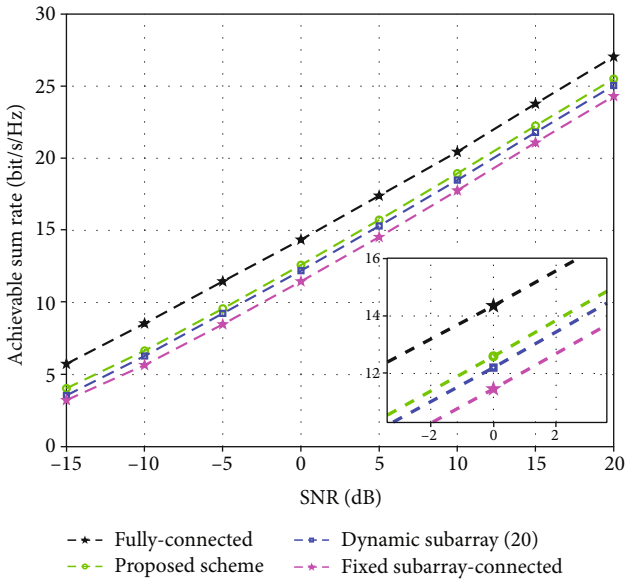

Figure 4: Spectral efficiency comparison for the mmWave MIMO system with $N_T = 128$, $N_R = 2$, $K = 2$, and $N_{RF} = 2$ RF chains.

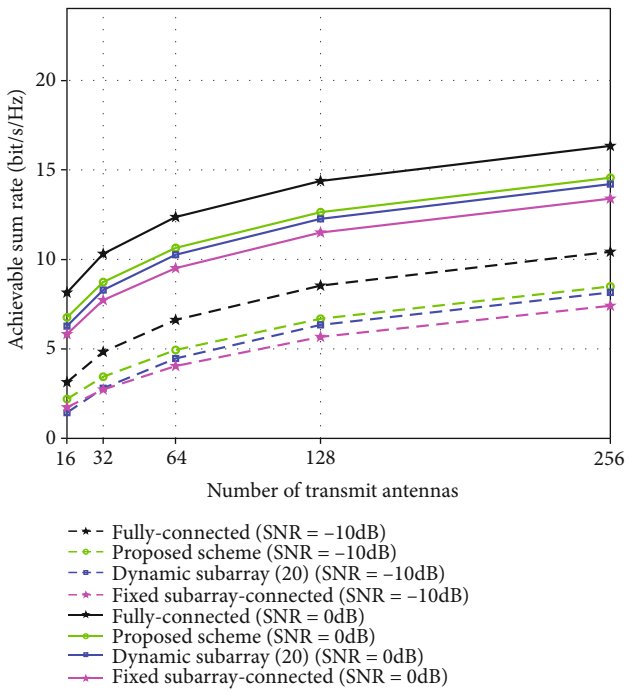

Figure 5: Spectral efficiency comparison for the mmWave MIMO system with different numbers of transmitting antennas.

In this paper, we use $P_{RF} = 250$mW [26] and $P_{PS} = 1$mW [27] in simulation, P_t is constrained to $\|\mathbf{F}_{RF}\mathbf{F}_{BB}\|_F^2 = K$. The energy efficiency comparison against the number of RF chains N_{RF} is shown in Figure 6, where $N_T = 128$, $N_R = 2$, and SNR = 0 dB. We can see that with

the increase of the number of RF chains, the energy efficiency gradually decreases, which is consistent with the theoretical analysis. Moreover, it is clear that the dynamic subarray-connected architectures have higher energy efficiency than the fully connected architectures. In addition, compared with the existing dynamic subarray schemes, the energy efficiency of the proposed scheme is improved by 3.5% on average.

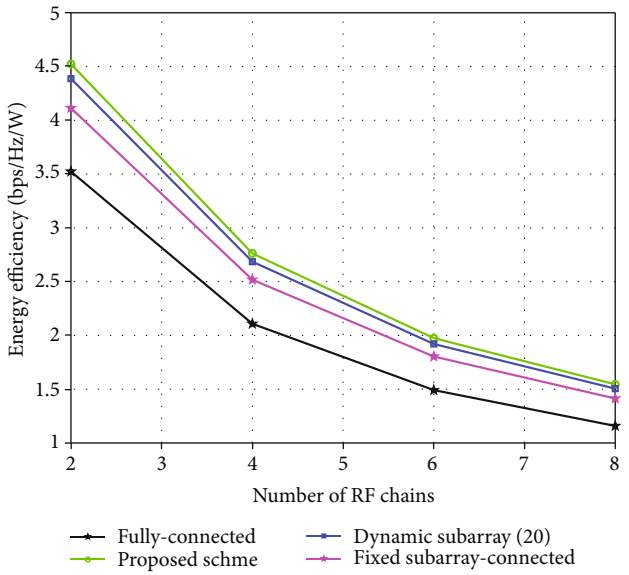

Figure 6: Energy efficiency comparison against the numbers of RF chains, where $N_T = 128$, SNR = 0 dB, $N_R = 2$, and $K = 2$.

Figure 7 shows the energy efficiency comparison against the number of transmitting antennas of BS, where $N_T = 16$, 32, 64, 128, and 256, SNR = 0 dB, $N_{RF} = 2$, and $K = 2$. As the number of base station antennas increases, the energy efficiency first increases and then decreases, especially for fully connected architectures, which are faced with rapid performance degradation. In addition, the proposed schemes achieve better energy efficiency than existing dynamic subarray schemes and can maintain a high and stable energy efficiency between 64 and 256 antennas.

5.3. User Fairness Analysis. As an indicator of the allocation of shared resources, fairness is widely used in various fields, for example, data collection in cognitive radio networks [28, 29] and data transfer in wireless communication systems. In a multiuser communication system, it is important to ensure that each user has access to roughly the same data transfer rate. In Section 4, we introduce user selection to provide better service for a small number of users, where it is important to ensure fairness among users. In order to investigate the fairness of each user, we introduce the Jain fairness index [30]. The Jain fairness index is a very effective measure of distributive fairness. Jain fairness index defines fairness among multiple users as

$$J(\mathbf{R}) = \frac{\left(\sum_{k=1}^{K} R_k\right)^2}{\left(K\sum_{k=1}^{K} R_k^2\right)}, \tag{28}$$

where $J(\mathbf{R})$ is the coefficient of fairness between K users, $J(\mathbf{R}) \in [1/K, 1]$. According to the definition of the Jain

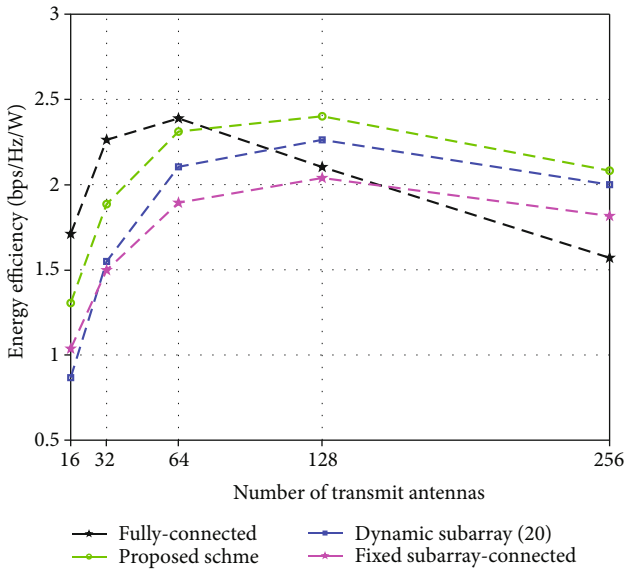

Figure 7: Energy efficiency comparison against the numbers of transmit antennas, where SNR = 0 dB, $N_R = 2$, and $K = 2$.

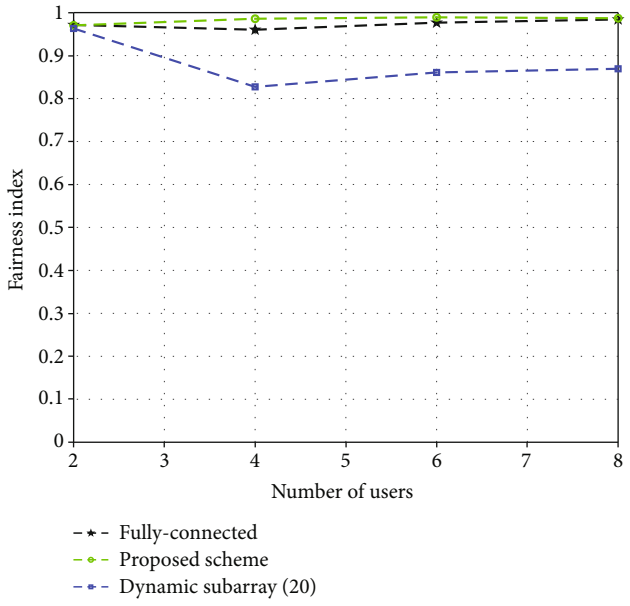

Figure 8: Fairness index comparison against the numbers of users K, where $N_T = 128$, $N_R = 2$, and SNR = −10 dB.

fairness index, if the value of $J(\mathbf{R})$ tends to $1/K$, the fairness is worse; on the other hand, if the value of $J(\mathbf{R})$ tends to 1, the fairness is better. In Figure 8, we compared the fairness of different schemes with different numbers of users K, where $N_T = 128$, SNR = −10 dB, and $N_R = 2$. We observe that our proposed scheme can make the fairness index close to 1 under the different number of users. However, the fairness index of the existing dynamic subarray schemes [20] decreases with the increase of the number of users.

6. Conclusion

In this paper, we propose a new antenna-partitioning algorithm and a multiuser hybrid precoding scheme for the dynamic subarray of multiuser mmWave massive MIMO systems. The idea is to ensure that each user has the same opportunity to obtain the optimal antenna according to the maximum channel gain of the selected user. Then, we design the hybrid precoding with high performance for dynamic subarray architecture. Simulation results show that the proposed scheme in this paper can make the spectrum efficiency closer to the fully connected architectures and the energy efficiency closer to the traditional subconnected architectures. Moreover, the scheme proposed in this paper, especially at low SNR, is more advanced than the existing dynamic subarray schemes. In terms of user fairness, our scheme can almost make every user reach the same achievable rate. For future work, we are interested to evaluate performance in the dynamic subarray architecture with uniform planar arrays (UPAs) and under imperfect channel state information.

Data Availability

The data used to support the findings of this study are available from the corresponding author upon request.

Conflicts of Interest

The authors declare no conflicts interest regarding the publication of paper.

Acknowledgments

This work was supported in part by the National Natural Science Foundation of China under Grant 61871466 and in part by the Key Science and Technology Project of Guangxi under Grant AB19110044.

References

[1] T. S. Rappaport, S. Sun, R. Mayzus et al., "Millimeter wave mobile communications for 5G cellular: it will work!," *IEEE Access*, vol. 1, pp. 335–349, 2013.

[2] S. Rangan, T. S. Rappaport, and E. Erkip, "Millimeter-wave cellular wireless networks: potentials and challenges," *Proceedings of the IEEE*, vol. 102, no. 3, pp. 366–385, 2014.

[3] O. E. Ayach, S. Rajagopal, S. Abu-Surra, Z. Pi, and R. W. Heath, "Spatially sparse precoding in millimeter wave MIMO systems," *IEEE Transactions on Wireless Communications*, vol. 13, no. 3, pp. 1499–1513, 2014.

[4] J. Zhao, F. Gao, W. Jia, S. Zhang, S. Jin, and H. Lin, "Angle domain hybrid precoding and channel tracking for millimeter wave massive MIMO systems," *IEEE Transactions on Wireless Communications*, vol. 16, no. 10, pp. 6868–6880, 2017.

[5] R. Méndez-Rial, C. Rusu, N. González-Prelcic, and R. W. Heath, "Dictionary-free hybrid precoders and combiners for mmWave MIMO systems," in *2015 IEEE 16th International Workshop on Signal Processing Advances in Wireless Communications (SPAWC)*, pp. 151–155, Stockholm, Sweden, 2015.

[6] X. Yu, J. Shen, J. Zhang, and K. B. Letaief, "Alternating minimization algorithms for hybrid precoding in millimeter wave

MIMO systems," *IEEE Journal of Selected Topics in Signal Processing*, vol. 10, no. 3, pp. 485–500, 2016.

[7] W. Ni, X. Dong, and W. Lu, "Near-optimal hybrid processing for massive MIMO systems via matrix decomposition," *IEEE Transactions on Signal Processing*, vol. 65, no. 15, pp. 3922–3933, 2017.

[8] Y. Wang and W. Zou, "Low complexity hybrid precoder design for millimeter wave MIMO systems," *IEEE Communications Letters*, vol. 23, no. 7, pp. 1259–1262, 2019.

[9] X. Gao, L. Dai, S. Han, I. Chih-Lin, and R. W. Heath, "Energy-efficient hybrid analog and digital precoding for mmWave MIMO systems with large antenna arrays," *IEEE Journal on Selected Areas in Communications*, vol. 34, no. 4, pp. 998–1009, 2016.

[10] Y. Liu, Q. Feng, Q. Wu, Y. Zhang, M. Jin, and T. Qiu, "Energy-efficient hybrid precoding with low complexity for mmWave massive MIMO systems," *IEEE Access*, vol. 7, pp. 95021–95032, 2019.

[11] Y. Chen, D. Chen, T. Jiang, and L. Hanzo, "Millimeter-wave massive MIMO systems relying on generalized sub-array-connected hybrid precoding," *IEEE Transactions on Vehicular Technology*, vol. 68, no. 9, pp. 8940–8950, 2019.

[12] D. H. N. Nguyen, L. B. Le, T. Le-Ngoc, and R. W. Heath, "Hybrid MMSE precoding and combining designs for mmWave multiuser systems," *IEEE Access*, vol. 5, pp. 19167–19181, 2017.

[13] X. Gao, L. Dai, Y. Sun, S. Han, and I. Chih-Lin, "Machine learning inspired energy-efficient hybrid precoding for mmWave massive MIMO systems," in *2017 IEEE International Conference on Communications (ICC)*, pp. 1–6, Paris, 2017.

[14] J. Chen, "Energy-efficient hybrid precoding design for millimeter-wave massive MIMO systems via coordinate update algorithms," *IEEE Access*, vol. 6, pp. 17361–17367, 2018.

[15] D. Zhang, Y. Wang, X. Li, and W. Xiang, "Hybrid beamforming for downlink multiuser millimetre wave MIMO-OFDM systems," *IET Communications*, vol. 13, no. 11, pp. 1557–1564, 2019.

[16] X. Zhu, Z. Wang, L. Dai, and Q. Wang, "Adaptive hybrid precoding for multiuser massive MIMO," *IEEE Communications Letters*, vol. 20, no. 4, pp. 776–779, 2016.

[17] S. Park, A. Alkhateeb, and R. W. Heath, "Dynamic subarrays for hybrid precoding in wideband mmWave MIMO systems," *IEEE Transactions on Wireless Communications*, vol. 16, no. 5, pp. 2907–2920, 2017.

[18] L. Zhang, L. Gui, Q. Qin, and Y. Tu, "Adaptively-connected structure for hybrid precoding in multi-user massive MIMO systems," in *2018 IEEE 29th Annual International Symposium on Personal, Indoor and Mobile Radio Communications (PIMRC)*, pp. 1–7, Bologna, Italy, 2018.

[19] X. Jing, L. Li, H. Liu, and S. Li, "Dynamically connected hybrid precoding scheme for millimeter-wave massive MIMO systems," *IEEE Communications Letters*, vol. 22, no. 12, pp. 2583–2586, 2018.

[20] J. Jiang, Y. Yuan, and L. Zhen, "Multi-user hybrid precoding for dynamic subarrays in mmWave massive MIMO systems," *IEEE Access*, vol. 7, pp. 101718–101728, 2019.

[21] A. Alkhateeb, G. Leus, and R. W. Heath, "Limited feedback hybrid precoding for multi-user millimeter wave systems," *IEEE Transactions on Wireless Communications*, vol. 14, no. 11, pp. 6481–6494, 2015.

[22] Z. Cai, Y. Duan, and A. G. Bourgeois, "Delay efficient opportunistic routing in asynchronous multi-channel cognitive radio networks," *Journal of Combinatorial Optimization*, vol. 29, no. 4, pp. 815–835, 2015.

[23] Q. Chen, Z. Cai, L. Cheng, and H. Gao, "Low-latency data aggregation scheduling for cognitive radio networks with non-predetermined structure," *IEEE Transactions on Mobile Computing*, p. 1, 2020.

[24] L. Liang, W. Xu, and X. Dong, "Low-complexity hybrid precoding in massive multiuser MIMO systems," *IEEE Wireless Communications Letters*, vol. 3, no. 6, pp. 653–656, 2014.

[25] D. H. Nguyen and T. Le-Ngoc, "MMSE precoding for multiuser MISO downlink transmission with non-homogeneous user SNR conditions," *EURASIP Journal on Advances in Signal Processing*, vol. 2014, Article ID 85, 2014.

[26] P. V. Amadori and C. Masouros, "Low RF-complexity millimeter-wave beamspace-MIMO systems by beam selection," *IEEE Transactions on Communications*, vol. 63, no. 6, pp. 2212–2223, 2015.

[27] W. Croswell, "Antenna theory, analysis, and design," *IEEE Antennas and Propagation Society Newsletter*, vol. 24, no. 6, pp. 28-29, 1982.

[28] Z. Cai, S. Ji, J. He, and A. G. Bourgeois, "Optimal distributed data collection for asynchronous cognitive radio networks," in *2012 IEEE 32nd International Conference on Distributed Computing Systems*, pp. 245–254, Macau, China, 2012.

[29] Z. Cai, S. Ji, J. He, L. Wei, and A. G. Bourgeois, "Distributed and asynchronous data collection in cognitive radio networks with fairness consideration," *IEEE Transactions on Parallel and Distributed Systems*, vol. 25, no. 8, pp. 2020–2029, 2014.

[30] A. B. Sediq, R. H. Gohary, R. Schoenen, and H. Yanikomeroglu, "Optimal tradeoff between sum-rate efficiency and Jain's fairness index in resource allocation," *IEEE Transactions on Wireless Communications*, vol. 12, no. 7, pp. 3496–3509, 2013.